

## Magnetic phase diagram and possible Lifshitz critical point in UPd<sub>2</sub>Si<sub>2</sub>

T. Plackowski, D. Kaczorowski, and J. Sznajd

*Institute of Low Temperature and Structure Research, Polish Academy of Sciences, P.O. Box 1410, PL-50-950 Wrocław, Poland*

(Received 20 March 2011; published 31 May 2011)

High-quality single crystals of UPd<sub>2</sub>Si<sub>2</sub> have been studied by means of heat capacity and magnetization measurements. The obtained data has yielded a  $H$ - $T$  phase diagram that significantly differs from those reported before in the literature. The main finding is identification of a multicritical point that seemingly exhibits Lifshitz characteristics.

DOI: [10.1103/PhysRevB.83.174443](https://doi.org/10.1103/PhysRevB.83.174443)

PACS number(s): 75.30.Kz, 75.30.Sg, 65.40.Ba, 05.10.Cc

### I. INTRODUCTION

The concept of a Lifshitz point (LP) was introduced in 1975 by Hornreich, Luban, and Shtrikman (Ref. 1). By definition LP is a special multicritical point in the  $H$ - $T$  phase diagram, which divides a continuous transition line between disordered and ordered phases into two segments, such that on the first part a transition is observed to uniform (commensurate) phase, while on the second part the transition occurs to some modulated (incommensurate) phase. In other words, LP is a point where the three phases—disordered, commensurate, and incommensurate—meet and the respective boundary lines join with a common tangent. The modulation wave vector  $\mathbf{Q}$  of the incommensurate phase varies continuously along the transition line. If the commensurate phase is ferromagnetic, the modulation vector continuously goes to zero as LP is approached; in other cases  $\mathbf{Q}$  goes to a nonzero value of  $Q_c$  which characterizes a uniform phase (e.g.,  $Q_c = 1$  for an antiferromagnetic phase and  $Q_c = \frac{2}{3}$  for a ferrimagnetic  $++-$  phase).<sup>2</sup>

Spatially modulated systems are very common in nature; modulated phases of various types have been observed in hundreds ferroelectric and magnetic crystals. Phase diagrams of these systems sometimes reveal multicritical points, which separate a high-temperature disordered phase and low-temperature commensurate and incommensurate phases. In a few cases the presence of a Lifshitz point has been suggested. Among nonmagnetic systems, the existence of LP has been established for example in uniaxial ferroelectrics Sn<sub>2</sub>P<sub>2</sub>(Se<sub>*x*</sub>S<sub>*1-x*</sub>)<sub>6</sub> (Ref. 3). As regards magnetic compounds, an archetypal example is the manganese monophosphide MnP for which the Lifshitz-type critical behavior has been comprehensively studied.<sup>4-9</sup> For a few other magnetic systems the LP concept has been extended to triple points, in which two<sup>10</sup> or even all three<sup>11</sup> incoming transition lines are of the first order. However, such an extension is clearly at odds with the main feature of the Lifshitz point, i.e., its critical behavior. For this reason, to date MnP remains recognized as the only example of a magnetic system, in which the conventional LP critical behavior has been evidenced unambiguously near the confluence of the paramagnetic phase with the ordered ferromagnetic and modulated phases.

The present work on the ternary uranium silicide UPd<sub>2</sub>Si<sub>2</sub> has been motivated by data reported in the literature<sup>12-15</sup> that indicated the presence of a triple point on the  $H$ - $T$  phase diagram. Although the available results for the phase boundaries near this point seem to be inconsistent with

the conventional LP scenario (the phase transition between paramagnetic and commensurate phases has been suggested to be of the first order), we have decided to reinvestigate the magnetic properties of the compound. UPd<sub>2</sub>Si<sub>2</sub> crystallizes with the body-centered tetragonal ThCr<sub>2</sub>Si<sub>2</sub>-type crystal structure (space group  $I4/mmm$ ).<sup>12</sup> It exhibits complex magnetic behavior with four distinct magnetic phases in its  $H$ - $T$  phase diagram.<sup>13-15</sup> In zero magnetic field, the compound orders antiferromagnetically at  $T_N = 136$  K with an incommensurate longitudinal sine wave (ICLSW) that propagates along the crystallographic  $c$  axis.<sup>13,15</sup> The propagation vector  $\mathbf{Q} = (00q_z)$ , initially determined to be equal to  $q_z = 0.731$  (Ref. 13), was then found to vary continuously with decreasing the temperature from  $q_z = 0.71$  at  $T_N$  to  $q_z = 0.74$  at  $T_t = 108$  K (Ref. 15). At  $T_t$ , the magnetic structure changes to a commensurate one, describable by the propagation vector  $\mathbf{Q} = (001)$  (Refs. 13,15). The latter structure is of a simple AFI type, where the ferromagnetically ordered layers of uranium atoms alternate antiferromagnetically along the  $c$  axis with a sequence  $+-+-$ . In both zero-field phases, the uranium magnetic moment amounts to  $2.3(1) \mu_B$  (Ref. 13). In a magnetic field stronger than 1.9 T, applied parallel to the fourfold axis, a different magnetic structure gets stabilized that is commensurate with the crystal lattice and defined by the propagation vector  $\mathbf{Q} = (002/3)$  (Ref. 14). The amplitude of that longitudinal spin wave (LSW) is  $3.0(3) \mu_B$  (Ref. 14). Notably, in each of the four phases the uranium magnetic moment is oriented along the tetragonal axis, which is a consequence of very strong uniaxial magnetocrystalline anisotropy.

In this paper, we report on our reinvestigation of the  $H$ - $T$  phase diagram of UPd<sub>2</sub>Si<sub>2</sub>, focused mainly on a hypothetical occurrence of a Lifshitz-type instability at the point of merging of the ICLSW, LSW, and paramagnetic (P) phases in strong magnetic fields. Interestingly, the derived magnetic phase diagram considerably differs in its low-temperature part from those hitherto published in the literature.<sup>14,15</sup>

### II. EXPERIMENTAL DETAILS

A single crystal of UPd<sub>2</sub>Si<sub>2</sub> was grown from the stoichiometric mixture of the elements (U 99.8 at.%, Pd 99.999 at.%, and Si 99.9999 at.%) by the Czochralski pulling method in a tetra-arc furnace under high-purity Ti-gettered argon atmosphere. The obtained ingot was 3 mm in diameter and 30 mm in length. It was then wrapped with Ta foil and heat treated in an evacuated quartz tube at 900 °C for two weeks.

Quality of the product was verified by means of x-ray powder diffraction (XRD) measurements (Stoe diffractometer with Cu  $K\alpha$  radiation) and energy dispersive x-ray (EDX) analysis (Phillips 515 scanning electron microscope equipped with an EDAX PV 9800 spectrometer). The XRD pattern, obtained on a powder specimen prepared from a pulverized fragment of the annealed crystal, was easily indexed using the FULLPROF program<sup>16</sup> within a simple body-centered tetragonal unit cell with the lattice parameters close to those reported before.<sup>12,13,15</sup> Microprobe examination of a few polished cross sections of the crystalline rod revealed homogeneous single-phase material with the composition equal to the ideal one (within an experimental accuracy). Hence, from a large part of the ingot several specimens were cut using a wire saw, suitable for measuring the physical properties along the main crystallographic axes.

As a nonmagnetic counterpart to  $UPd_2Si_2$ , a polycrystalline sample of  $ThPd_2Si_2$  was prepared by arc-melting the constituents (Th purity 99.8 at.%, purities of the other elements as given above) in a copper-hearth furnace installed inside a glove box filled with ultrapure argon gas with continuously controlled partial pressures of  $O_2$  and  $H_2O$  to be lower than 1 ppm. The button was flipped over and remelted several times to ensure good homogeneity. The weight losses after the final melting were negligible (less than 0.2%). No subsequent heat treatment was applied to the sample. The product, analyzed by means of XRD and EDX methods (equipment as described above), was found to be single phase with the expected tetragonal  $ThCr_2Si_2$ -type crystal structure.

Magnetic measurements were carried out in the temperature range from 1.71 to 300 K and in applied magnetic fields up to 5 T using a superconducting quantum interference device (SQUID) magnetometer (Quantum Design MPMS 5). Moreover, the magnetization of single-crystalline  $UPd_2Si_2$  was measured over the temperature interval 2–180 K and in magnetic fields up to 9 T applied along the  $c$  axis (Quantum Design PPMS-9 platform). Heat capacity measurements were performed in the temperature range 0.35–300 K using a heat-pulse technique (Quantum Design PPMS-9). Furthermore, heat capacity studies were made for  $UPd_2Si_2$  in external magnetic fields up to 13 T applied along the tetragonal axis. For these experiments, performed using an ac technique with the temperature slowly scanned (1 K/min) from 160 K down to 20 K and then back to 160 K, a homemade heat-flow calorimeter was utilized, installed inside a commercial cryostat (Oxford Instrument TESLATRON). The same equipment was used to study the isothermal magnetocaloric effect in  $UPd_2Si_2$ . Slow sweeps (0.2 T/min) of magnetic fields from 13 T down to zero were made at several temperatures in the range 20–140 K. In these measurements the single crystal was oriented with its  $c$  axis along the magnetic field. A general description of the experimental method used and details on the employed setup can be found in Refs. 17–19.

### III. EXPERIMENTAL RESULTS

#### A. Heat capacity

Figure 1 displays the temperature dependence of the specific heat of single-crystalline  $UPd_2Si_2$ . The  $C(T)$  curve

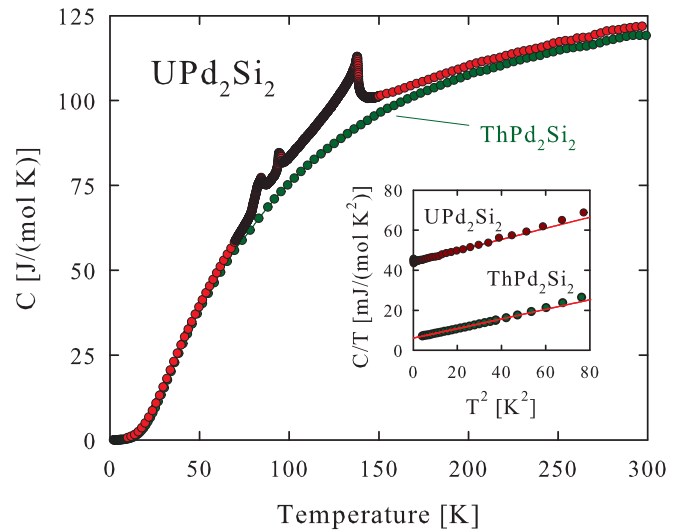


FIG. 1. (Color online) Temperature dependence of the specific heat of single-crystalline  $UPd_2Si_2$  (measured on heating the sample) compared with that of polycrystalline  $ThPd_2Si_2$ . Inset:  $C/T$  ratio as a function of  $T^2$  plotted for both compounds. The solid lines emphasize a linear behavior.

is dominated by a sharp  $\lambda$ -like anomaly at  $T_N = 138.4(4)$  K and two smaller anomalies at  $T_1 = 96.5(5)$  K and  $T_2 = 85(1)$  K, superimposed on a usual sigmoid-shaped function. Unambiguously, the singularity observed at  $T_N$  is due to the onset of the antiferromagnetically ordered state revealed by the neutron diffraction experiments<sup>13,15</sup> and evidenced in the published heat capacity<sup>15,20</sup> and electrical resistivity<sup>15,21</sup> data. In turn, the specific-heat features occurring at  $T_1$  and  $T_2$ , which likely manifest order-order magnetic phase transitions (see below), have not been reported in the literature so far. Furthermore, at odds with the previous results,<sup>13,15</sup> no singularity in  $C(T)$  is seen in Fig. 1 at  $T_t = 108$  K, where the transition from the ICLSW phase to the AFI phase was reported. Similarly, there is no hint of any phase transition near 40 K, which was evidenced in early neutron studies on a powder sample,<sup>12</sup> yet not confirmed in subsequent investigations on single crystals.<sup>13–15</sup>

Below 6 K, the specific heat of  $UPd_2Si_2$  can be described using a formula  $C(T) = \gamma T + \beta T^3$ , where the first term accounts for the electronic contribution and the second one stands for the sum of the phonon and antiferromagnetic magnon contributions:  $\beta = \beta_{ph} + \beta_m$ . A least-squares fit of this formula to the experimental data (see the inset to Fig. 1) yielded  $\gamma = 44.3(7)$  mJ/(mol K<sup>2</sup>) and  $\beta = 0.2767(4)$  mJ/(mol K<sup>4</sup>). In order to derive  $\beta_m$  it was assumed that the phonon spectrum in  $UPd_2Si_2$  can be approximated by that in  $ThPd_2Si_2$ . Applying similar data analysis (see the inset to Fig. 1) one finds for the nonmagnetic Th counterpart  $\gamma = 6.1(2)$  mJ/(mol K<sup>2</sup>) and  $\beta_{ph} = 0.2394(9)$  mJ/(mol K<sup>4</sup>). The latter value implies for  $UPd_2Si_2$  the parameter  $\beta_m = 0.0373$  mJ/(mol K<sup>4</sup>). From the relation  $\beta_{ph} = r \frac{12\pi^4}{5} \Theta_D^{-3}$  ( $r$  is a number of atoms in a formula unit), the Debye temperature in both compounds can be estimated as  $\Theta_D = 344$  K. The Sommerfeld coefficient derived for the U-based compound is larger by  $\gamma_{5f} = 38$  mJ/(mol K<sup>2</sup>) than that found for  $ThPd_2Si_2$ , which can be attributed to the contribution due to  $5f$  electrons.

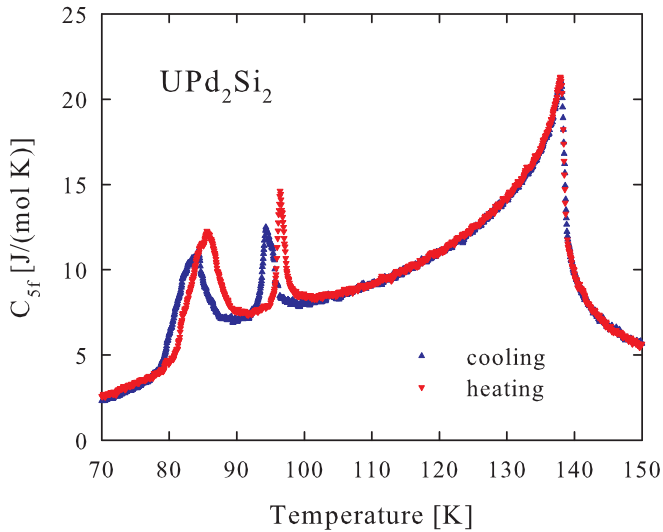


FIG. 2. (Color online) Temperature variations of the excess specific heat due to  $5f$  electrons in single-crystalline  $\text{UPd}_2\text{Si}_2$ , measured with increasing and decreasing temperature.

At higher temperatures, the specific heat of  $\text{ThPd}_2\text{Si}_2$  nearly traces that of  $\text{UPd}_2\text{Si}_2$ , except for the vicinity of the phase transitions, thus proving that in both compounds the phonon contribution to the specific heat is nearly same. Hence, the difference between the two curves, shown in Fig. 2, represents a sum of the electronic and magnetic contributions to  $C(T)$  of the U-based silicide. The latter component might generally comprise the heat capacity due to the phase transitions and the Schottky specific heat due to crystalline field effect. However, in the case of  $\text{UPd}_2\text{Si}_2$ , the latter contribution seems negligible, as the above-derived  $\gamma_{5f}T$  term fully accounts for the observed rising “background” in  $C_{5f}(T)$ . As may be inferred from Fig. 2, the phase transitions at  $T_1$  and  $T_2$  exhibit considerable thermal hysteresis. The critical temperatures, defined as nodes in the temperature derivative of  $C(T)$ , are  $T_1 = 96.5(5)$  K and  $T_2 = 85(1)$  K for heating, and  $T_1 = 94.2(7)$  K and  $T_2 = 83(2)$  K for cooling the sample while the specific-heat data were collected. This finding strongly suggests that both transitions are of the first-order (discontinuous) nature. On the contrary, the peak at  $T_N = 138.4(4)$  K is independent of the thermal regime of measurement, as can be expected for the second-order (continuous) transition from the paramagnetic to the magnetically ordered state.

Figure 3 displays the specific heat of  $\text{UPd}_2\text{Si}_2$  measured in the region of the phase transitions in magnetic fields applied along the crystallographic  $c$  axis. The main finding is a strong field dependence of  $T_1$  that rapidly shifts toward higher temperatures with rising magnetic field. Simultaneously, the peak in  $C(T)$  becomes more pronounced, while the width of its thermal hysteresis diminishes. An opposite behavior is seen for  $T_2$ ; namely, the transition quickly moves to lower temperatures, the related hysteresis widens, and the anomaly in  $C(T)$  cannot be discerned already in fields above 2 T. In contrast, the value of  $T_N$  appears hardly dependent on the applied magnetic field. With increasing the field strength the lambda-shaped specific heat anomaly sharpens, especially when the transition at  $T_1$  merges with that at  $T_N$ , which happens near  $\mu_0H = 10$  T. Based on the experimental data presented in Fig. 3 one may

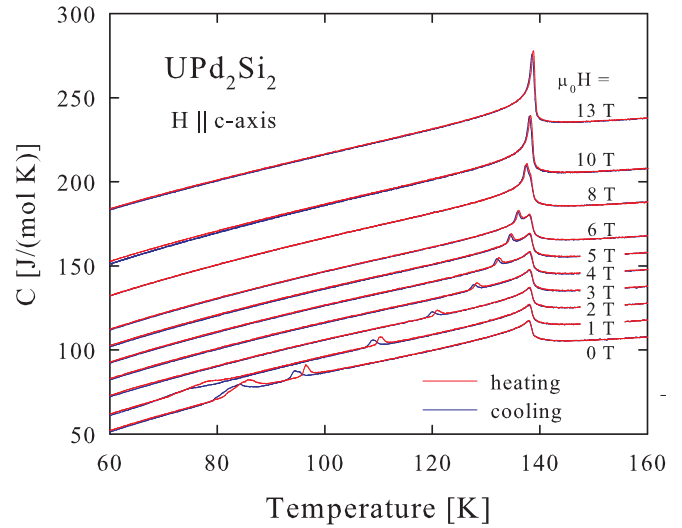


FIG. 3. (Color online) Temperature variations of the specific heat of single-crystalline  $\text{UPd}_2\text{Si}_2$ , measured with increasing and decreasing temperature in an external magnetic field of different strength, applied along the crystallographic  $c$  axis. For the sake of clarity, the curves taken in finite fields were systematically shifted upward [by  $k \times 10$  J/(mol K<sup>2</sup>), where  $k$  is the magnetic field strength in teslas].

construct the magnetic phase diagram, which is discussed in Sec. IV.

### B. Isothermal magnetocaloric effect

The results of the isothermal magnetocaloric coefficient measurements, performed in magnetic fields oriented along the fourfold axis of the  $\text{UPd}_2\text{Si}_2$  single crystal, are summarized in Fig. 4. At temperatures below  $T_2$  (see panel *a*), the coefficient  $M_T$  forms a pronounced negative minimum that shifts to stronger fields with decreasing the temperature. Initially, the shift is rather rapid, yet then becomes only slightly dependent on the temperature. The negative sign of  $M_T$  is a characteristic feature of antiferromagnets, in which application of external magnetic field results in an increment of the magnetic entropy  $\Delta S(H) = -\int_0^H \frac{M_T}{T} dH$  (Ref. 18). With further increasing the field one observes a tendency for changing the sign of  $M_T$  to positive (the most obvious sign change is seen for the isotherm taken at 69.9 K, where  $M_T$  is positive above about 2 T). Positive magnetocaloric effect is obviously a consequence of decreasing entropy upon decreasing field, as expected for ferromagnets.<sup>19</sup> Thus, the dips in  $M_T(H)$  define the boundary between the phases III and II (cf. Fig. 6), and the different signs of  $M_T$  reflect the antiferromagnetic and ferrimagnetic character of these two phases, respectively (see the discussion in Sec. IV).

The  $M_T(H)$  isotherms displayed in Fig. 4(b) have positive values in the entire range of the magnetic field strength. The distinct sharp peaks manifest a first-order transition from phase I, which forms in low fields, to phase II induced by magnetic field (see Fig. 6). Remarkably, no similar anomaly is seen on the curve measured at 89.8 K, in concert with the

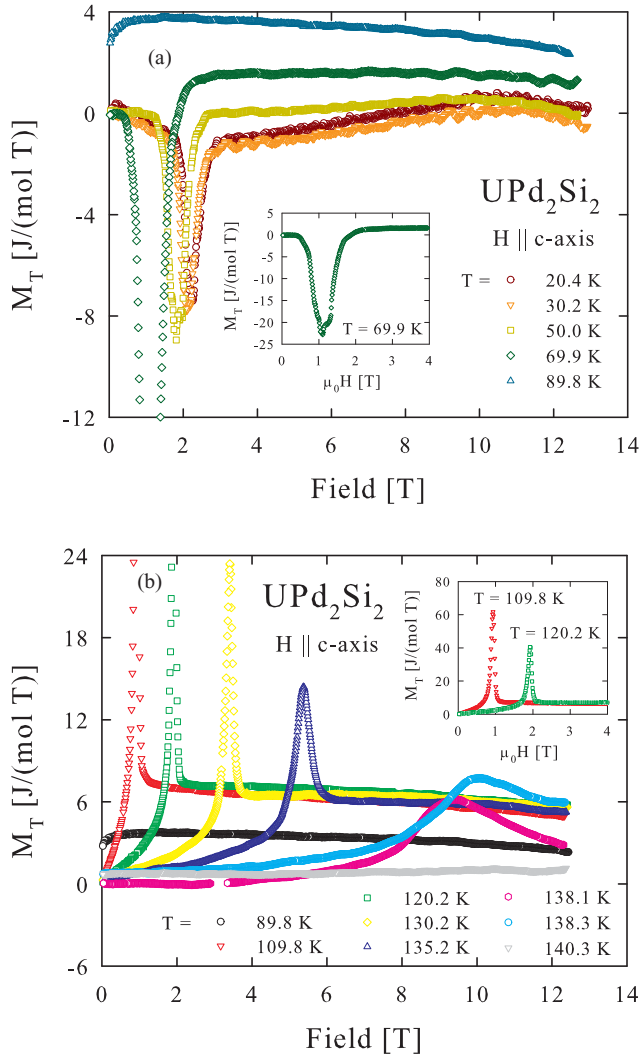


FIG. 4. (Color online) Magnetic field variations of the isothermal magnetocaloric coefficient of single-crystalline  $\text{UPd}_2\text{Si}_2$ , measured at a few different temperatures from the range (a) 20–90 K and (b) 90–150 K. The magnetic field was applied along the crystallographic  $c$  axis, and the experimental data were taken with decreasing the field strength from 13 T down to zero. For the sake of clarity the vertical axes were somewhat cut, and the insets present the affected curves in their full shape in fields below 4 T.

occurrence of the ferrimagnetic phase II in all fields down to 0 T.

It is worthwhile noting that isotherms taken at 138.1 and 138.3 K exhibit entirely different behavior from the other ones. Instead of sharp peaks found at lower temperatures, the two  $M_T(H)$  curves form broad maxima located above 9 T. As discussed below (see Sec. IV), the latter anomalies signal a transition from the paramagnetic to the ordered state (phase II), and their shape is indicative of the second-order nature of this transition. In the paramagnetic region (represented by the curve measured at 140.3 K), the isothermal magnetocaloric coefficient of  $\text{UPd}_2\text{Si}_2$  is positive, small, and nearly independent of the magnetic field strength.

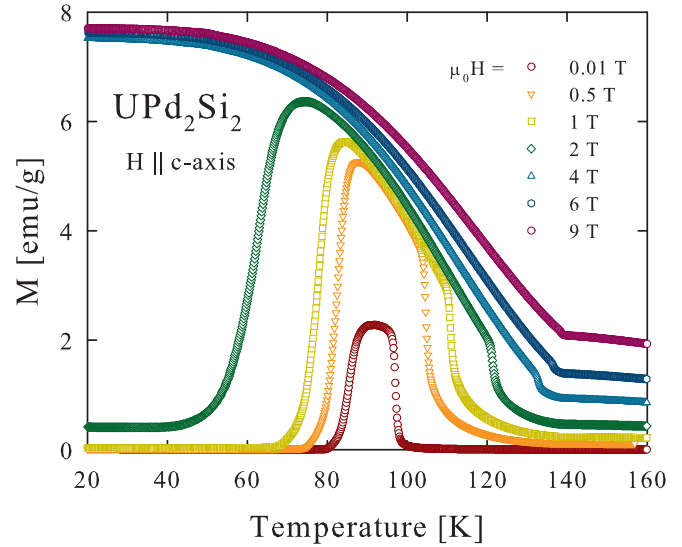


FIG. 5. (Color online) Temperature variations of the magnetization in single-crystalline  $\text{UPd}_2\text{Si}_2$  measured with increasing temperature in a few different external magnetic fields applied along the crystallographic  $c$  axis. Before each measurement the specimen was cooled down to 20 K in the applied field of a given strength.

### C. Magnetic properties

Figure 5 presents the magnetization curves taken for the single crystal of  $\text{UPd}_2\text{Si}_2$  with magnetic field oriented along the tetragonal  $c$  axis. In a weak magnetic field of 0.01 T,  $M(T)$  is dominated by a pronounced trapezoid-like feature located approximately between  $T_2$  and  $T_1$ . Both the shape and the magnitude of this anomaly suggest a ferromagnetic-like behavior in the compound just in this temperature interval, which separates the two regions of antiferromagnetic spin compensation. With increasing field strength, the ferromagnetic-like range gradually widens on the temperature scale; i.e.,  $T_2$  decreases and  $T_1$  increases. An abrupt qualitative change in the overall shape of  $M(T)$  occurs above  $\mu_0 H = 2$  T; namely, the anomaly at  $T_2$  cannot be distinguished anymore and the ferromagnetic-like region extends to 20 K, the terminal temperature in this experiment. The field variations of  $T_1$  and  $T_2$ , defined as singularities in the temperature derivatives  $dM/dT$ , are included on the  $H$ - $T$  phase diagram, shown in Fig. 6. Remarkably, neither the magnetization curves nor their derivatives provided any information on the phase transition to the paramagnetic state that takes place at  $T_N$ , as unambiguously established from the specific heat data.

In strong magnetic fields, the magnetization curves of  $\text{UPd}_2\text{Si}_2$  show at low temperatures a ferromagnetic-like saturation (see Fig. 5). The magnetization measured at 20 K in a field of 9 T amounts to 7.7(1) emu/g that corresponds to the magnetic moment  $\mu_s$  of about 0.7  $\mu_B$ . The latter value is similar to that reported in Ref. 15 as the saturation magnetization at a temperature of 1.7 K in steady magnetic fields up to 23 T. Furthermore, it is worth noting that  $\mu_s$  is nearly one-third of the amplitude of the spin wave in the LSW phase,<sup>14</sup> which nicely corresponds to the  $++-$  sequence of the uranium moments along the  $c$  axis (see discussion below).

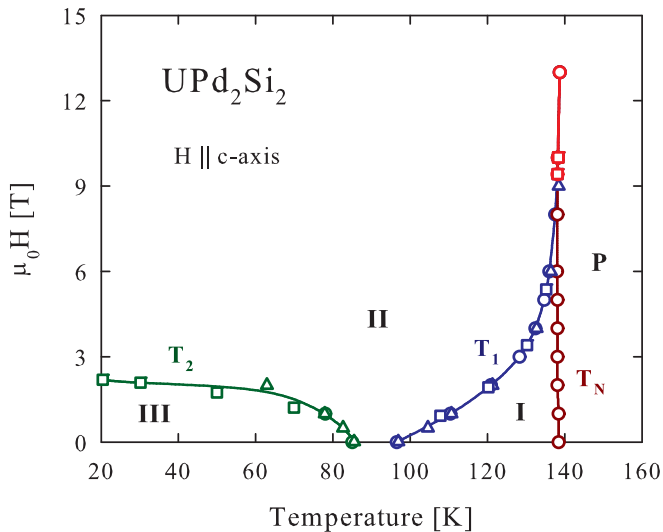


FIG. 6. (Color online) Magnetic phase diagram of UPd<sub>2</sub>Si<sub>2</sub>, constructed from the specific heat (circles), magnetocaloric (squares), and magnetization (triangles) data collected in external magnetic fields directed along the crystallographic *c* axis. The experiments were carried out as described in the captions of Figs. 3, 4, and 5.

#### IV. DISCUSSION

##### A. Magnetic phase diagram

Based on the obtained specific heat, magnetocaloric, and magnetization data, one may construct for UPd<sub>2</sub>Si<sub>2</sub> the *H-T* phase diagram displayed in Fig. 6. It comprises three different magnetic phases (I, II, and III) besides the paramagnetic phase (P). The magnetic behavior of the compound, observed below *T*<sub>1</sub>, suggests a ferromagnetic-like character of the phase II (cf. the magnetization and the isothermal magnetocaloric coefficient data), whereas the phases I and III seem to have purely antiferromagnetic nature. Invoking the results of neutron diffraction experiments,<sup>13–15</sup> one may associate the phase I with the incommensurate longitudinal spin wave (ICLSW) structure defined by the propagation vector  $q_z \approx 0.73$ , the phase II with the commensurate longitudinal spin wave (LSW) characterized by  $q_z = 2/3$ , and the phase III with the simple antiferromagnetic (AFI) spin arrangement given by  $q_z = 1$  (see the Introduction). It is worth noting that the phase II has a ferrimagnetic character, which results from an uncompensated magnetic moment in the sequence  $++-$  of the uranium moments directed along the *c* axis and ferromagnetically coupled within the tetragonal *a-b* planes.<sup>14,15</sup>

Although the above interpretation of the different magnetic phases in the measured single crystal of UPd<sub>2</sub>Si<sub>2</sub> seems most appropriate as it adheres to the hitherto published *H-T* data, this assignment still needs verification by means of additional neutron diffraction experiments. This is because of significant differences between the zero-field bulk properties of the compound established in the present work and those given in the literature.<sup>13–15,20,21</sup> Whereas the Néel temperature  $T_N = 138.4$  K, derived from the specific-heat data [no anomaly at this temperature occurs in  $M(T)$  in accord with the previous findings<sup>13,14,21</sup>], is reasonably close to  $T_N = 136$  K reported before, clearly no hint at any phase boundary can be seen in

$C(T)$  at  $T_i = 108$  K, in striking contrast to the results presented in Refs. 15,20,21. On the other hand, the specific heat peaks due to the first-order transitions at  $T_1 = 96.5$  K and  $T_2 = 85$  (values obtained while heating the specimen) are reported here for the first time. These two temperatures define the stability range of the ferromagnetic-like phase II (distinctly seen also in the magnetization data), which has not been reported to exist in  $\mu_0 H = 0$ . However, it is worth recalling that in all the previous papers<sup>13–15,20,21</sup> the authors discussed some ferromagnetic contribution to the magnetization in their single crystals, which was interpreted either as a tiny admixture of the LSW phase to the AFI phase or as being due to the presence of an unknown impurity. Remarkably, the ferromagnetic signal was always observed exclusively between about 80 and 100 K, i.e., in the interval of existence of phase II in zero field, discovered in this work (see Fig. 6). Interestingly, the ferromagnetic behavior in this temperature range was reported also in early studies on polycrystalline samples of UPd<sub>2</sub>Si<sub>2</sub> (Refs. 22,23).

Faced with such notably dissimilar magnetic behavior of UPd<sub>2</sub>Si<sub>2</sub>, found in this study and that reported in the literature, one should pose a question on a possible origin of the observed discrepancies. A straightforward explanation may refer to differences in the real crystal structure (stoichiometry, atom disorder, strain, etc.) of the samples investigated. It is well known that some tiny deviations from the ideal 1 : 2 : 2 composition (most probable here being a deficiency in the Pd content) may have a profound influence on the physical properties, as can be best exemplified by recalling the case of an archetypal heavy-fermion superconductor CeCu<sub>2</sub>Si<sub>2</sub> (Ref. 24), which crystallizes with the same crystal structure as UPd<sub>2</sub>Si<sub>2</sub>. On the other hand, sample-dependent properties of the  $UT_2X_2$  intermetallics (*T* represents a *d*-electron transition metal, and *X* = Si or Ge) have been recognized as originating in different heat treatments of poly- and single-crystalline material after casting.<sup>25</sup> In this context it should be emphasized that all the hitherto published results for single crystals of UPd<sub>2</sub>Si<sub>2</sub> were obtained on specimens cut from as-grown Czochralski-pulled ingots. The only exception was the magnetic susceptibility data reported in Ref. 15, which were taken on an annealed crystal. Interestingly, the latter specimen showed ferromagnetic-like humps around 95 and 80 K (in a field of 0.01 T), i.e., near *T*<sub>1</sub> and *T*<sub>2</sub> identified in the present study. It seems likely that heat treatment induces some changes in the crystal structure of the single-crystalline material. Rather obvious effects would be thermal-driven release of strains, structural disorder, and/or stacking faults. The most distinct one would be an annealing-induced phase transformation between two derivatives of the tetragonal BaAl<sub>4</sub>-type structure. The majority of the  $RT_2X_2$  phases (*R* stands for a lanthanoid or actinoid) crystallize either in the body-centered ThCr<sub>2</sub>Si<sub>2</sub>-type structure (space group  $I4/mmm$ ) or in the primitive CaBe<sub>2</sub>Ge<sub>2</sub>-type structure (space group  $P4/nmm$ ). However, a few compounds, e.g., CeIr<sub>2</sub>Si<sub>2</sub> (Ref. 26) and UCo<sub>2</sub>Ge<sub>2</sub> (Ref. 27), are known to form in both modifications, i.e., the low-temperature body-centered polymorph and the primitive high-temperature one, which can be stabilized by means of appropriate annealing. Interestingly, these two structural variants exhibit distinctly different physical properties.<sup>27,28</sup> By analogy, one may speculate that a similar scenario applies to UPd<sub>2</sub>Si<sub>2</sub>. Precise crystal structure refinements, performed on both as-cast and annealed

single crystals, are indispensable to prove this challenging hypothesis.

Strong support for the above interpretation of the differences in the zero-field magnetic behavior in UPd<sub>2</sub>Si<sub>2</sub> single crystals, in terms of possible changes in the crystal structure induced by heat treatment, can be found in Ref. 29, where the results of x-ray scattering measurement are quoted. For a well-annealed single crystal (with annealing conditions very similar to those applied in the present work), the following sequence of successive phase transitions was established while cooling the sample below the Néel temperature  $T_N = 136$  K. In the temperature interval 136–95 K, the studied crystal exhibited an incommensurate longitudinal spin wave (ICLSW) with the propagation vector component  $q_z$  increasing with decreasing temperature from 0.71 to 0.74. In the temperature range 125–105 K, this spin wave coexisted with another incommensurate one that had a fixed propagation vector  $q_z = 0.711$ , whereas in the interval 108–105 K a third antiferromagnetic phase, identified as a simple commensurate structure of the AFI type, was observed. The latter phase was found to accompany the ICLSW phase down to  $T_1 = 95$  K. At the latter temperature, both of these phases disappeared and the compound became ferrimagnetic due to the formation of a commensurate longitudinal spin wave (LSW) structure with  $q_z = 2/3$ . Eventually, at  $T_2 = 85$  K, the LSW phase transformed into the AFI phase that persisted down to the lowest temperatures studied. In the entire ordered state the magnetic moments were found to be carried by the uranium atoms only, and oriented parallel (or antiparallel) to the crystallographic  $c$  direction. Obviously, the above picture of successive phase transitions, the magnetic character of the particular phases, and even the values of the critical temperatures  $T_N$ ,  $T_1$ , and  $T_2$  are all in excellent agreement with the findings reported for UPd<sub>2</sub>Si<sub>2</sub> in the present paper.

## V. PHENOMENOLOGY

### A. $H$ - $T$ phase diagram

The main features of physical systems exhibiting spatially modulated structures are usually described by means of the axial next-nearest neighbor Ising (ANNNI) model.<sup>31</sup> However, in order to explain an occurrence and sequences of magnetically ordered states in real systems more complicated models are required. Such a modification of the ANNNI approach has been proposed by Selke *et al.* (Ref. 32), who considered additional axial interactions to third-neighbor layers. In turn, Plumer (Ref. 30) has derived a classical Heisenberg version of this model with third-neighbor layer interactions (A3NNH). In the framework of the molecular field approximation (MFA), the model describes a variety of sequences of different magnetic phases, among them the transitions experimentally observed in UPd<sub>2</sub>Si<sub>2</sub>, i.e.,  $P \rightarrow I \rightarrow II \rightarrow III$  and  $P \rightarrow II$  (see Fig. 6). However, within the A3NNH model there is no temperature or field dependence of the incommensurate phase wave vector  $\mathbf{Q}$  and all the transitions except for  $P \rightarrow I$  are of the first order. The A3NNH approach with both the easy-axis anisotropy and the nearest-neighbor biquadratic exchange interactions has been proposed by Mailhot *et al.* (Ref. 33) as a model for UNi<sub>2</sub>Si<sub>2</sub>, an isostructural counterpart to UPd<sub>2</sub>Si<sub>2</sub>. The authors concluded that due to biquadratic exchange the vector  $\mathbf{Q}$  varies with

temperature; however the sequence of phases  $II \rightarrow III \rightarrow I \rightarrow P$ , experimentally observed in UNi<sub>2</sub>Si<sub>2</sub>, could not be explained by that model at least within MFA. Eventually, such a sequence of the magnetic phases has been reproduced within a subsequent extension proposed by Muraoka (Ref. 34), who considered  $S = 1$  A3NNI with a three-site four-spin interaction.

The most recent calculations made for UPd<sub>2</sub>Si<sub>2</sub> are those by Honma *et al.* (Ref. 15), who have confined themselves to the original ANNNI model and calculated a  $H$ - $T$  phase diagram, which for some values of the exchange parameters “roughly consists of four regions” observed experimentally. However, because of the lack of experimental data in the middle range of the magnetic field strength, the authors were not able to investigate the triple point where the three phases I, II, and P meet. In particular, they could not resolve the question whether the phase transition from the paramagnetic phase to the ordered phases I and II keeps at the triple point its second-order character, as predicted within the conventional Lifshitz point scenario.<sup>1</sup>

As is clear from the above remarks, no well-established microscopic theory of the magnetic behavior in UPd<sub>2</sub>Si<sub>2</sub> is available. The most often used one is based on the ANNNI model and its extensions concerning the range of competing interactions, the spin value or/and the higher order spin interactions. For lack of strong physical arguments, the only justification for the choice of the interaction form is its efficiency in reproducing the magnetic phase diagram and the character of the several phase transitions. Unfortunately, any description of the entire  $H$ - $T$  diagram established experimentally requires so many fitting parameters that such an approach becomes rather useless. For this reason, we decided to confine ourselves exclusively to the vicinity of the triple point where the three phases—P, ICSW, and LSW—meet (see Fig. 6). Based on the similarity between the high-temperature parts of the phase diagram of UPd<sub>2</sub>Si<sub>2</sub> and that established for UAs<sub>0.97</sub>Se<sub>0.03</sub> (Refs. 35–37), we have attempted to analyze the  $P \rightarrow II$  transition in terms of the six-layer model, applied previously to the latter compound.<sup>37</sup> The relevant Hamiltonian reads

$$\mathcal{H} = -j_1 \sum_{i,j,n} S_i^n S_i^{n+1} - j_2 \sum_{i,j,n} S_i^n S_i^{n+2} - k \sum_{i,j,n} S_i^n S_j^n S_i^{n+1} S_j^{n+1} - h \sum_{i,n} S_i^n, \quad (1)$$

where  $S_i^n$  denotes an Ising spin  $S = \pm 1$  in the  $n$ th layer,  $k$  is the four-spin interaction parameter, while  $h$  stands for the reduced magnetic field. In order to describe the phases  $(+ - + -)$ ,  $(+ + -)$ , and P experimentally observed in UPd<sub>2</sub>Si<sub>2</sub>, one should consider at least six layers (of course, such a six-layer model cannot describe any incommensurate phase). Denoting the magnetization of the  $n$ th layer by  $m_n = \langle S_i^n \rangle$  and introducing the variables<sup>37</sup>

$$m = \frac{1}{6} \sum_{n=1}^6 m_n, \quad \phi_2 = m_1 + m_2 + m_3 - m_4 - m_5 - m_6, \\ \phi_3 = m_1 - m_3, \quad \phi_4 = m_2 - m_6, \quad \phi_5 = m_1 - m_4, \quad (2) \\ \phi_6 = m_3 - m_6,$$

one can define the ferrimagnetic order parameter

$$\phi_f = \phi_3 = \phi_4. \quad (3)$$

Within this model, the MFA free energy for the P  $\rightarrow$  II phase transition takes the form

$$f_{\text{MFA}} = \frac{1}{3} (18Jm^2 + 54km^2 - 2J\phi_f^2 + 8km\phi_f^3 + 2k\phi_f^4) - 3t \lg \left[ 64 \cosh^4 \frac{27h + 54Jm + 54km^3 - 9J\phi_f + 9km\phi_f^2 + 5k\phi_f^3}{54t} + \cosh^2 \frac{27h + 2(3m + \phi_f)[9J - k(9m^2 - 3m\phi_f - 2\phi_f^2)]}{54t} \right], \quad (4)$$

where  $J = j_1 + j_2$ , and  $t$  denotes the reduced temperature. In the frame of the original ANNNI model ( $k=0$ ),  $f_{\text{MFA}}$  can be expanded with regard to the order parameter  $\phi_f$  as follows:

$$f_L = 6Jm^2 - t \lg \left( 64 \cosh^6 \left[ \frac{h + 2Jm}{2t} \right] \right) + \frac{J(T \tanh^2 \left[ \frac{h+2Jm}{2t} \right] - J^2 - 4Jt)}{6t} \phi_f^2 - \frac{J^3 \tanh \left[ \frac{h+2Jm}{2t} \right] (\tanh^2 \left[ \frac{h+2Jm}{2t} \right] - 1)}{54t^2} \phi_f^3 + \dots \quad (5)$$

For the symmetry reasons, the third-order term in the ferrimagnetic order parameter  $\phi_f$  does not vanish in the above expansion, which means, according to the Landau theory, that the state (point) with  $\phi_f = 0$  is not a stable one, and consequently the system does not undergo a continuous phase transition. As seen in Eq. (5), the third-order term is equal to zero only for  $h = 0$  or  $t = 0$ . However, if one takes into account the four-spin interaction  $k \neq 0$  the third-order term yields

$$r = -A^3 J^3 - 18A^2 Jkmt + 18kmt(J + 8t) + A(J^3 - 12kt^2), \quad (6)$$

where

$$A = \tanh \left[ \frac{h + 2Jm + 2km^3}{2t} \right]. \quad (7)$$

Now, the additional tuning parameter  $k$  allows the coefficient  $r$  to reach a vanishing-point at the transition temperature, and the conditions for the existence of the critical point can be written as

$$\begin{aligned} r = 0, \quad -J^2 - 4Jt + J^2 A^2 &= 0, \\ 6m(J + 6km^2) - 3(J + 3km^2)A &= 0. \end{aligned} \quad (8)$$

Remarkably, these conditions define the Landau isolated critical point.<sup>38</sup> The coordinates  $t_c$  and  $h_c$  of such a point are shown in Fig. 7 as functions of the four-spin interaction parameter  $k$  assuming  $J = -1$ . Apparently, in these conditions, the Landau critical point exists for any value of  $k$  in the range  $0 < k < 0.675$ . This means that the ANNNI model supplemented by a specific type of the additional interactions (e.g., the four-spin interaction) can yield the special isolated critical point. It should be recalled in this context that in a general approach the Landau expansion of the free energy contains a nonremovable cubic term, which excludes any possibility for the transition line to exhibit the continuous-order character.

## B. Lifshitz point

The most intriguing conjecture that can be formulated from the  $H$ - $T$  phase diagram derived for UPd<sub>2</sub>Si<sub>2</sub> is a possible occurrence of the tricritical Lifshitz instability at  $T = T_L \simeq 138.1$  K and  $\mu_0 H = \mu_0 H_L \simeq 9$  T, i.e., at the point of merging the phases I, II, and P. Indeed, in concert with the definition of the conventional Lifshitz point,<sup>1</sup> the two ordered phases are incommensurate (ICLSW) and commensurate (LSW), respectively, and all three phase boundaries meet at  $(H_L, T_L)$  with common tangents (see Fig. 6). Most importantly, the specific heat anomaly at the transition from the paramagnetic to the ordered state seems to preserve its lambda-shaped character also in fields  $H > H_L$  (cf. Fig 3), which likely manifests the second-order nature of the P  $\rightarrow$  II transition. Furthermore, the jump in the magnetization at the ICLSW  $\rightarrow$  LSW transition

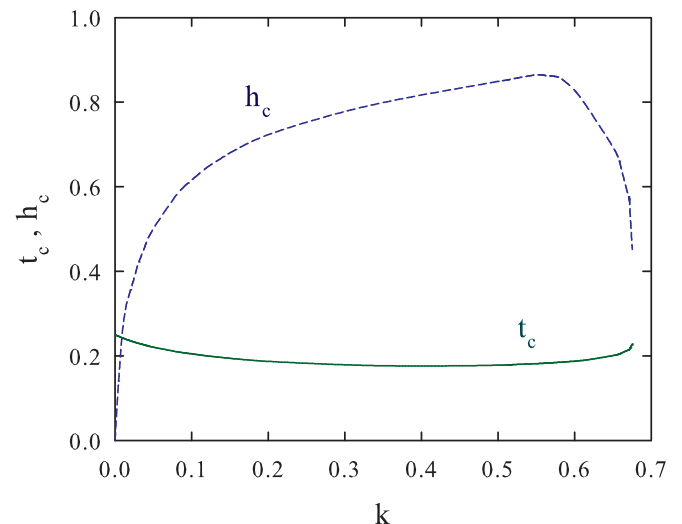


FIG. 7. (Color online) Coordinates  $(t_c, h_c)$  of the Landau critical isolated point as functions of the four-spin interaction parameter  $k$ .

clearly decreases with increasing magnetic field strength and seems to vanish for  $H \rightarrow H_L$  (cf. Fig. 5). Also this behavior hints at the continuous character of the transition at  $(H_L, T_L)$ .

An important prerequisite for the occurrence of the conventional Lifshitz point concerns the modulation vector  $\mathbf{Q}$  of the incommensurate phase, which should approach at LP the commensurate phase value. In the case of  $\text{UPd}_2\text{Si}_2$ , the vector  $\mathbf{Q} = (00q_z)$  that just below  $T_N$  amounts to  $q_z = 0.71$  in zero magnetic field<sup>29</sup> should vary with increasing field strength to reach  $q_z = \frac{2}{3}$  of the LSW phase. Although detailed neutron diffraction data taken in the vicinity of  $(H_L, T_L)$  are lacking, some support for such a behavior in  $\text{UPd}_2\text{Si}_2$  can be derived from the results shown in Ref. 14; namely,  $q_z$  indeed decreases with increasing  $\mu_0 H$  toward the commensurate phase value that describes the  $(++-)$  ferrimagnetic phase.

Based on the above arguments,  $\text{UPd}_2\text{Si}_2$  seems to be the second example, after MnP, where the conventional LP instability occurs. In contrast to systems such as  $\text{NaNO}_2$  (Ref. 10) or  $\text{UAs}_{1-x}\text{Se}_x$  (Refs. 37,39) in which the transition from the paramagnetic state to the commensurate (ferro or ferri) phase is of the first order, the experimental data presented in this paper favor the second-order nature of the latter phase boundary. However, it should be stressed that even if the  $\text{P} \rightarrow \text{II}$  transition would appear discontinuous, as predicted by the classical ANNNI approach to the phase transition in a nonzero field between the paramagnetic phase and the Ising type ferrimagnetic  $++-$  phase, accidentally in  $\text{UPd}_2\text{Si}_2$  the point at which the I and II ordered phases meet the paramagnetic phase can be at least the isolated critical point. It seems that at this stage of research any speculation is useless as to what type of interactions (four-spin, biquadratic, three-site, effectively temperature dependent, etc.) are responsible for the critical character of the para-ferri phase transition. Undoubtedly, further experimental work is necessary to shed more light on the nature of the magnetic interactions in this interesting material.

## VI. SUMMARY

In striking dissonance with quite extensive theoretical development of the concept of the Lifshitz point instability, made since the original paper by Hornreich *et al.* (Ref. 1), experimentally, LP as “a multicritical point whose critical behavior is strikingly different from any other,”<sup>1</sup> has so far been identified in one magnetic system only, namely, in MnP. In our opinion, a good candidate for the occurrence of the Lifshitz-type behavior is  $\text{UPd}_2\text{Si}_2$ . The  $H$ - $T$  phase

diagram of this compound comprises three ordered phases I, II, and III, characterized by the incommensurate longitudinal spin wave, commensurate ferrimagnetic-like, and simple antiferromagnetic structures, respectively.<sup>14,15</sup> In this paper, based on the heat capacity, isothermal magnetocaloric effect, and magnetization data measured with the magnetic field applied parallel to the easy magnetization direction (tetragonal axis), the  $H$ - $T$  phase diagram has been constructed, which significantly differs from that published in the literature.<sup>14,15</sup> In zero field, instead of the phase transition at 108 K between the incommensurate and antiferromagnetic phases, reported in the previous papers, we have observed two successive first-order phase transitions between the incommensurate and ferrimagnetic phases and between the ferrimagnetic and antiferromagnetic phases that occur at 96.5 K and 85 K, respectively. As a consequence, we have not observed a triple point at  $T \sim 107$  K,  $H \sim 1.9$  T, in which three ordered phases I, II, and III meet.<sup>15</sup> On the other hand, we have gained from our experimental data novel information on the other tricritical point of merging the phases P, I, and II. Remarkably, the latter singularity seems to possess the fingerprints of the conventional Lifshitz point, as hitherto established exclusively for MnP. Further comprehensive experimental and theoretical studies are necessary to verify this hypothesis. Of prime importance is determination by means of neutron diffraction of whether the propagation vector of the incommensurate phase  $\mathbf{Q}$  continuously goes to that of the commensurate ferrimagnetic phase while the triple point is approached. Furthermore, the temperature dependencies of the magnetization and the specific heat should be investigated in strong magnetic fields to unambiguously define the order of the phase transition between the ferrimagnetic and paramagnetic phases near the triple point. It will also be worthwhile to study the critical behavior near the hypothetical Lifshitz point. In particular, the specific heat  $\alpha_L$  and magnetic susceptibility  $\gamma_L$  critical exponents, and first of all the wave vector exponent  $\beta_q$  (describing the approach to the commensurate phase value  $q_z = \frac{2}{3}$ ), should be measured across the phase boundary lines and compared with the theoretical predictions for the Lifshitz instability.<sup>1,40-42</sup>

## ACKNOWLEDGMENTS

The work was supported by the Ministry of Science and Higher Education under Research Grant No. N N202 193234.

<sup>1</sup>R. M. Hornreich, M. Luban, and S. Shtrikman, *Phys. Rev. Lett.* **35**, 1678 (1975).

<sup>2</sup>R. M. Hornreich, in *Magnetic Phase Transitions. Proc. of the Summer School*, Erice, Italy, July 1983 (Springer Verlag, Berlin, 1983), p. 40.

<sup>3</sup>Yu. M. Vysochanskii and V. Yu. Slivka, *Sov. Phys. Usp.* **35**, 123 (1992) and references therein.

<sup>4</sup>C. C. Becerra, Y. Shapira, N. F. Oliveira Jr., and T. S. Chang, *Phys. Rev. Lett.* **44**, 1692 (1980).

<sup>5</sup>Y. Shapira, C. C. Becerra, N. F. Oliveira Jr., and T. S. Chang, *Phys. Rev. B* **24**, 2780 (1981).

<sup>6</sup>R. H. Moon, J. M. Cable, and Y. Shapira, *J. Appl. Phys.* **52**, 2025 (1989).

<sup>7</sup>V. Bindilatti, C. C. Becerra, and N. F. Oliveira Jr., *Phys. Rev. B* **40**, 9412 (1989).

<sup>8</sup>C. C. Becerra, N. F. Oliveira Jr., and Y. Shapira, *J. Physique Coll.* **49**, C8895 (1988).

- <sup>9</sup>H. Yoshizawa, S. M. Shapiro, and T. Komatsubara, *J. Phys. Soc. Jpn.* **54**, 3084 (1985).
- <sup>10</sup>S. L. Qiu, M. Dutta, H. Z. Cummins, J. P. Wicksted, and S. M. Shapiro, *Phys. Rev. B* **34**, 7901 (1986).
- <sup>11</sup>I. Lukýanchuk, A. Jorio, and P. Saint-Gregoire, *Phys. Rev. B* **61**, 3147 (2000).
- <sup>12</sup>H. Ptasiwicz-Bak, J. Leciejewicz, and A. Zygmunt, *J. Phys. F* **11**, 1224 (1981).
- <sup>13</sup>B. Shemirani, H. Lin, M. F. Collins, C. V. Stager, J. D. Garrett, and W. J. L. Buyers, *Phys. Rev. B* **47**, 8672 (1993).
- <sup>14</sup>M. F. Collins, B. Shemirani, C. V. Stager, J. D. Garrett, H. Lin, W. J. L. Buyers, and Z. Tun, *Phys. Rev. B* **48**, 16500 (1993).
- <sup>15</sup>T. Honma, H. Amitsuka, S. Yasunami, K. Tenya, T. Sakakibara, H. Mitamura, T. Goto, G. Kido, S. Kawarazaki, Y. Miyako, K. Sugiyama, and M. Date, *J. Phys. Soc. Jpn.* **67**, 1017 (1998).
- <sup>16</sup>J. Rodriguez-Carvajal, *Physica B* **192**, 55 (1992).
- <sup>17</sup>T. Plackowski, Y. Wang, and A. Junod, *Rev. Sci. Instrum.* **73**, 2755 (2002).
- <sup>18</sup>T. Plackowski, D. Kaczorowski, and Z. Bukowski, *Phys. Rev. B* **72**, 184418 (2005).
- <sup>19</sup>T. Plackowski and D. Kaczorowski, *Phys. Rev. B* **72**, 224407 (2005).
- <sup>20</sup>T. Startseva, F. S. Razavi, H. Salamati, G. Quirion, and J. D. Garrett, *Phys. Rev. B* **58**, 113 (1998).
- <sup>21</sup>M. Barati, W. R. Datars, T. R. Chien, C. V. Stager, and J. D. Garrett, *Phys. Rev. B* **48**, 16926 (1993).
- <sup>22</sup>H. Ptasiwicz-Bak, J. Leciejewicz, and A. Zygmunt, *J. Phys. F* **11**, 1225 (1981).
- <sup>23</sup>T. T. M. Palstra, A. A. Menovsky, G. J. Nieuwenhuys, and J. A. Mydosh, *J. Magn. Magn. Mater.* **54-57**, 435 (1986).
- <sup>24</sup>F. Steglich, P. Gegenwart, C. Geibel, R. Helfrich, P. Hellmann, M. Lang, A. Link, R. Modler, G. Sparn, N. Büttgen, and A. Loidl, *Physica B* **223-224**, 1 (1996).
- <sup>25</sup>M. Kuznietz, *J. Phys. Condens. Matter* **17**, 3117 (2005), and references cited therein.
- <sup>26</sup>D. Niepmann and R. Pöttgen, *Intermetallics* **9**, 313 (2001).
- <sup>27</sup>T. Endstra, G. J. Nieuwenhuys, A. A. Menovsky, and J. A. Mydosh, *J. Appl. Phys.* **69**, 4816 (1991).
- <sup>28</sup>M. Mihalik, M. Diviš, and V. Sechovský, *Physica B* **404**, 3191 (2009).
- <sup>29</sup>D. Wermeille, C. Vettier, N. Bernhoeft, A. Stunault, S. Langridge, F. de Bergevin, F. Yakhou, E. Lidström, J. Flouquet, and P. Lejay, *Phys. Rev. B* **58**, 9185 (1998).
- <sup>30</sup>M. L. Plumer, *Phys. Rev. B* **50**, 13003 (1994).
- <sup>31</sup>P. Bak, *Rep. Prog. Phys.* **45**, 587 (1982); M. E. Fisher and D. A. Huse, *Melting, Localization, and Chaos* (Elsevier, Amsterdam, 1992), p. 259; W. Selke, *Modulated Structure Materials*, edited by T. Tsakalacos (Nijhoff, Dordrecht, 1984), p. 23.
- <sup>32</sup>W. Selke, M. Barreto, and J. Yeomans, *J. Phys. C* **18**, L393 (1985).
- <sup>33</sup>A. Mailhot, M. L. Plumer, A. Caille, and P. Azaria, *Phys. Rev. B* **45**, 10399 (1992).
- <sup>34</sup>Y. Muraoka, *Phys. Rev. B* **64**, 134416 (2001).
- <sup>35</sup>J. Rossat-Mignod, P. Burllet, S. Quezel, O. Vogt, and H. Bartholin, in *Crystalline Electric Field Effects in f-Electron Materials*, Proc. IV Int. Conf. on Crystal-Field and Structural Effects in f-Electrons Systems, Wrocław, Poland, 1981, edited by R. P. Guertin, W. Suski, and Z. Zolnierak (Plenum Press, New York, 1982).
- <sup>36</sup>O. Vogt and H. Bartholin, *J. Magn. Magn. Mater.* **29**, 291 (1982).
- <sup>37</sup>T. Plackowski, M. Matusiak, and J. Sznajd, *Phys. Rev. B* **82**, 094408 (2010).
- <sup>38</sup>L. D. Landau and E. M. Lifshitz, *Statistical Physics*, 2nd ed. (Pergamon, Oxford, 1969).
- <sup>39</sup>S. K. Sinha, G. H. Lander, S. M. Shapiro, and O. Vogt, *Phys. Rev. Lett.* **45**, 1028 (1980); *Phys. Rev. B* **23**, 4556 (1981).
- <sup>40</sup>D. Mukamel, *J. Phys. A* **10**, L249 (1977).
- <sup>41</sup>R. M. Hornreich and A. D. Bruce, *J. Phys. A* **11**, 595 (1978).
- <sup>42</sup>H. W. Diehl and M. Shpot, *Phys. Rev. B* **62**, 12338 (2000); M. Shpot and H. W. Diehl, *Nucl. Phys. B* **612** [FS], 340 (2001).